Crack Initiation and Propagation in Fiber-Glass Reinforced Mortars

Pascale Saba, Tulio Honorio, Omar-Ateeq Mahmood, and Farid Benboudjema

Abstract Reinforced cement-based rendering mortars are used as the protection layer in External Thermal Insulation Composite Systems (ETICS). Thermal insulations, when used in renovation, have a big impact on the reduction of CO_2 emissions. The interactions with the environment changing temperature and relative humidity lead to thermal and hygral strains, which when restrained, may lead to stresses that can attain the tensile strength of the material causing then the mortar cracking. The eventual penetration of water inside the cracks may cause the insulator to lose partially its efficiency and durability. Here, we focus on the cracking development in the reinforced mortar layer using experimental techniques. To understand the crack initiation and propagation in the reinforced mortar layer, and the role of the fiber-glass mesh as reinforcement inside the mortar, a new mechanical setup is developed. This setup is designed to perform 3-point bending tests using in-situ X-ray tomography. The latter allows observing the cracks inside the mortar sample shedding lights on the reinforcement mechanisms of the fiber-glass mesh and its impact on the initiation and the propagation of the cracks. The role of the mortar heterogeneities is also analyzed and information about cracks characteristics such as openings and lengths may be extracted.

Keywords Mortar · Cracking · 3-points bending · X-ray tomography · Fiber-glass

P. Saba (✉) · T. Honorio · F. Benboudjema
LMT - Laboratoire de Mécanique et Technologie, Université Paris-Saclay, ENS Paris-Saclay, CNRS, 91190 Gif-sur-Yvette, France
e-mail: pascale.saba@ens-paris-saclay.fr

P. Saba · O.-A. Mahmood
Département Thermique, Mécanique et Modélisation, Saint-Gobain Recherche Paris, Quai Lucien Lefranc, 93300 Aubervilliers, France

F. Kanavaris et al. (eds.), *International RILEM Conference on Early-Age and Long-Term Cracking in RC Structures*, RILEM Bookseries 31,
https://doi.org/10.1007/978-3-030-72921-9_6

1 Introduction

Final energy use in buildings led to direct emissions of 10 Gigatons of CO_2 in 2019 worldwide [1]. Buildings were, therefore, responsible for 28% of global energy emissions. In France, home and building heating systems are responsible for 45% of total French energy consumption and about 25% of Greenhouse gas emissions [2]. The objective of the French government is to attain carbon neutrality by 2050 and to collectively set as an ambition the renovation of 500,000 housing units per year, half of which are occupied by low-income households [2]. Covid-19 Crisis pushed the government to further investigate in the field of energetic renovation with "France Relance" project [3] that insists on the ecological and energetic transition as the main part of the economic growth.

Two types of thermal insulation can be used in renovation projects: (i) External Thermal Insulation Composite Systems (ETICS) and (ii) Internal Thermal Insulation Systems. The popularity of the ETICS technology grew due to its advantages regarding the internal counterpart. ETICS guarantee the reduction of the thermal bridges and greater thermal comfort due to the higher interior thermal inertia, providing a finished appearance similar to the traditional rendering. From the construction point of view, ETICS allow thinner exterior walls and increase the facades' durability. Three very relevant aspects in the construction industry must be added to the advantages above: low cost, ease of application, and the possibility to be installed without disturbing the building's dwellers, which is particularly important in refurbishment [4]. As shown in Fig. 1, the protection layer of the insulator, expanded polystyrene, in ETICS is a base coat, which is a rendering mortar reinforced with fiberglass mesh.

Like all cementitious materials, rendering mortars are subject to cracking. The interactions with the environment changing temperature and relative humidity lead to thermal and hygral strains, which when restrained, may lead to stresses that can attain the tensile strength of the material causing then the mortar cracking as in Fig. 2. This is problematic for two main reasons. On one hand, the eventual penetration of water

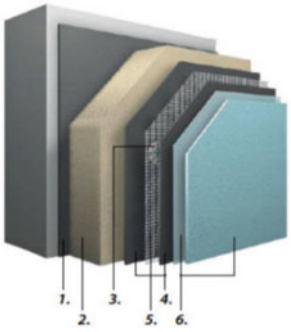

1. Adhesive
2. Thermal insulation material
3. Anchors (not mandatory)
4. Base-coat
5. Reinforcement, usually glass fiber mesh
6. Finishing layer: finishing coat with a key coat (optional) and/or decorative coat (optional)

Fig. 1 Typical system components in ETICS using anchors [5]

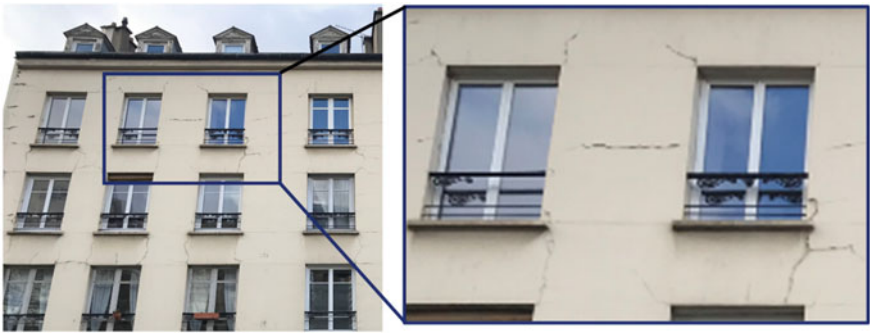

Fig. 2 Visible cracking on a facade

inside the cracks may cause the insulator to lose partially its efficiency and durability. On the other hand, the visible cracking on the newly renovated façades leads to unsatisfied clients which is an important marketing problem. Oriented and non-oriented cracking and visibility of joints are among the main anomalies encountered in ETICS [6–8]. The glass fiber mesh fabric is proposed as a solution for cracking in several types of applications including the base coat reinforcement for ETICS.

The reinforced cement composite used in ETICS is composed of (i) the mortar, which is a heterogeneous cement-based material containing three main phases at its mesoscale: cement paste matrix, sand particles, and porosity, and (ii) the fiber-glass mesh which is also a composite heterogeneous material containing three phases at its mesoscale: glass fibers, porosity, and coating. These heterogeneities present in the mortar, the porosity, the sand, or even the mesh can be the source of localization for cracks at the mesoscale. Nevertheless, cracking in the rendering mortar can also be initiated at the structure scale. Geometrical singularities, such as window corners and thermal joints, can be a source of localization of cracks.

Here, we focus on the mechanical characterization of the reinforced rendering mortar. The aim is to determine the main source of crack localization and crack propagation in the mortar in 3D, using X-ray tomography in an original setup. The tomography scans enable unveiling the role of heterogeneities with a characteristic size on the order of a hundred micrometers—namely, (macro)porosity, aggregates, and fiber-glass mesh—on crack localization and crack propagation in reinforced mortar. To the author's knowledge, it has never been done previously on this type of material.

2 Materials and Experimental Methods

2.1 Materials

In this study, 5 mm thickness prismatic reinforced mortar samples of 70 mm long and 12 mm large (see Fig. 3a) are tested in bending inside an X-ray tomograph. The mortar used in our samples is a commercial basecoat for ETICS. The fiber-glass mesh is also a commercial glass fiber mesh fabric (see Fig. 3b) that is specifically preconized for ETICS.

Three non-reinforced mortar samples ($4 \times 4 \times 16$ cm^3) were tested by 3-point bending at 28 days to determine its mechanical properties such as the Young modulus and the tensile strength. The experimental setup and procedure are described in [9]. The mortar has a Young modulus of 2.47 ± 0.34 GPa, and a tensile strength of 1.97 ± 0.04 MPa (mean value $\pm$ standard deviation for both parameters).

Mixing protocol for the mortar. The manufacturer of the basecoat recommends 6 L of water for 25 kg of mortar. He preconizes mixing the water and the premix using an electric hand mixer at low speed (500 rpm) for 3 min, then letting the mixture rests for 5–10 min before application.

In this study, some modifications have been made. The water/premix ratio is kept, but not the mixing protocol. This decision is justified by the non-repeatability of the procedure if using a hand mixer since the movement of the human hand or body can never be the same. To limit the variability related to human intervention, a stand electric mortar mixer (IBERMIX) is used.

Since the mixing speed of the stand mixer is limited, we decided to select the mixing protocol detailed in Table 1, after having studied the effects of mixing protocol on mortar's properties.

Curing conditions. After casting, the samples are protected from drying for 24 h until demolding using several layers of plastic film and a final layer of adhesive aluminum. After demolding, the samples are stored in a temperature and relative humidity-controlled room at 20 °C ± 1 °C and 60% ± 5% respectively. Weight loss of the samples is monitored.

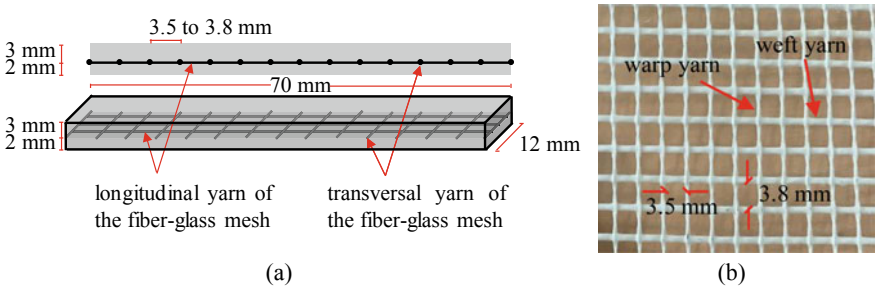

Fig. 3 **a** 2D and 3D representation of the fiber glass mesh reinforced mortar sample. **b** Glass-fiber mesh fabric structure

Table 1 Mixing protocol

Step	Speed [rpm]	Duration [s]
Mixing the premix before adding water	140	60
Mixing while progressively adding water	140	60
Mixing at high speed	300	90
Mixing with a trowel to scrape the sides	NA	60
Mixing at high speed	300	60
Leaving the mixture to "rest"	NA	5–10 min

2.2 Experimental Methods

To understand the crack initiation and propagation in the reinforced rendering mortar and the reinforcement mechanisms of the fiber-glass mesh, several specimens are tested using in-situ X-ray tomography. Specimens are loaded in 3-point and 4-point bending.

The rendering mortar is subject to drying shrinkage or hygral swelling in case of a decrease or increase of the relative humidity of the surrounding air, respectively. Only the external surface of the mortar will exchange humidity with the surrounding air. Therefore, only the external surface of the mortar will shrink or swell causing a "curling" effect [10] of the mortar as shown in Fig. 4. The "curling" effect puts the mortar under bending load. Similar resulting loads can be obtained with restrained thermal strains in case of an increase or decrease of the surrounding external temperatures caused by a difference in the thermal expansion coefficient between the mortar and the expanded polystyrene. For these reasons, we opted for bending tests as a primarily loading on the reinforced rendering mortar samples.

As mentioned in Sect. 1, cracks can be initiated on two different levels:

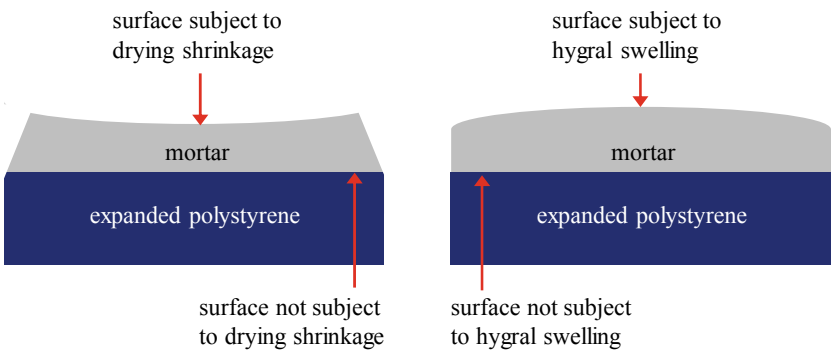

Fig. 4 "Curling" effect in the rendering mortar in ETICS

i. On the mesoscale, where the heterogeneities of the mortar (porosity, sand particles, and the mesh) are the only source of stress concentration.
ii. On the structural scale, where the geometrical singularities such as window corners and thermal joints take the lead of the stress concentration and crack initiation.

And so, 4-point bending tests, on one hand, are representative of the cracking that takes place on facades without geometrical singularities where the heterogeneities of the mortar are the main crack initiators. On the other hand, 3-point bending tests are representative of the cracking that occurs on the geometrical singularities where the stress is localized.

In-situ X-ray tomography, for instance, is the tool that will permit the visualization of the crack in the volume of the specimen. A 3D crack monitoring is possible at different times of the tests. It is also possible to extract information as crack openings, crack length, etc.

X-ray tomography. X-ray tomography is a non-destructive technique that allows obtaining a three-dimensional image. It is an imaging technique that generates a data set, called tomogram, which is a three-dimensional representation of the structure. Each three-dimensional point in the tomogram is called a voxel.

In a tomography experiment (see Fig. 5), 3D information is gathered by acquiring a series of 2D images while rotating the sample typically between 0 and 360°. Polychromatic X-rays from a micro-focus X-ray source are used to probe the specimen and an X-ray camera is used to record the X-ray transmission radiograph. To generate the tomogram, a series of radiographs are collected at different viewing angles by rotating the specimen. This set of radiographs, called projection data, are processed with a reconstruction algorithm to generate the tomogram of the specimen.

X-ray tomography is based on the variations in absorption coefficient along the path of the X-ray beam. The absorption coefficient is linked to the density and the atomic number of the different materials that the beam encounters as it passes through the sample. This is translated by Beer-Lambert law that links the transmitted beam intensity to material attenuation coefficient.

In case of monochromatic X-ray beams, the transmitted beam intensity is calculated as:

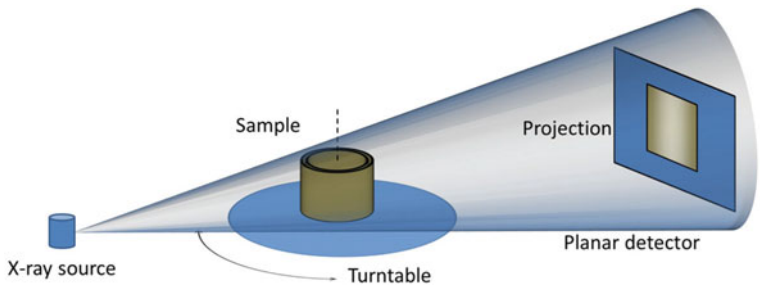

Fig. 5 Principal components of conventional X-ray tomography system (cone-beam example) [11]

$$I = I_0 \cdot exp\left[\sum_i (-\mu_i x_i)\right] \tag{1}$$

where I_0 and I are the X-ray intensities of the incident and transmitted beams, μ_i denotes the linear attenuation coefficient and x_i the linear extent of the *ith* material traversed by the beam. In case of polychromatic beams containing a large spectrum of energies, the beam flux is much higher and the exposure time is reduced. The transmitted beam intensity becomes:

$$I = \int I_0(E) \cdot exp\left[\sum_i (-\mu_i(E) x_i)\right] dE \tag{2}$$

where both I_0 and μ_i are related to the energy E of the incident beam.

Mechanical test assembly. In this contribution, we will be focusing on the 3-point bending setup. The latter is detailed in Fig. 6.

The specimen in this particular 3-point bending setup, unlike in traditional ones, is inclined. This change is what allowed us to obtain better quality images since the X-ray beam is traversing a smaller distance in the "scanned zone" shown in Fig. 6 compared to the total length of the specimen in case of a non-inclined bending setup. This can be related to the Eqs. (1) and (2) whereas the larger x_i, the smaller the transmitted beam intensity I.

Note that supports 2, 3, 4, and 5 of Fig. 6 are made of PMMA (*poly(methyl methacrylate))* which has a density of about 1185 kg.m^{-3}. The density of the mortar being 1323 $\pm$ 5 kg.m^{-3} (mean value $\pm$ standard deviation) making it denser than the PMMA. Thus, the PMMA is more X-ray transparent.

Plate 7 in Fig. 6 is directly fixed on a 100 N load cell that will put the plate in an upward movement, hence the load is being transmitted to the specimen by the lower supports.

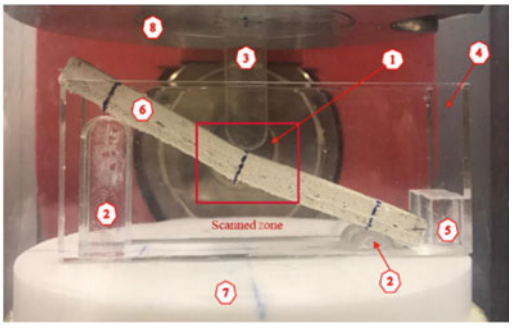

1. X-ray source
2. Lower supports
3. Upper support
4. Side supports
5. Longitudinal support
6. Specimen
7. Plate in an upward movement
8. Fixed plate

Fig. 6 3-point bending mechanical assembly

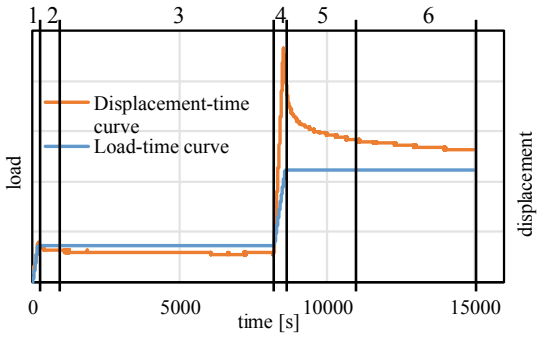

1. Load until contact
2. Relaxation period
3. First scan at a slightly deformed stage
4. Load until the first crack
5. Relaxation period
6. Second scan at cracked stage

Fig. 7 The schematic course of the test described with the load vs. time and displacement versus time curves

The test is controlled by the displacement of the plate 7 at a rate of 1 $\mu m.s^{-1}$. The advantage of using a displacement controlled test compared to a load controlled one is that the former allows getting the post-peak curve and prevents creep strains during the scans that will complicate the analysis of displacement fields related to cracking. Two scans are done to compare the cracked stage of the sample to its slightly deformed elastic stage. Before each scan, a pause period is preferred to allow the material to relax. This relaxation period prevents differential strains (for instance between viscous cement paste and elastic aggregates) that will occur during the scan hence limiting the blurred image. The in-situ inclined 3-point bending test is divided into 6 phases that are detailed in Fig. 7.

3 Experimental Results and Discussions

3.1 Experimental Results

Thanks to the advanced technology of the X-ray in-situ tests, reconstruction algorithms, and image processing algorithms, we had access to the 3D volume of the cracked sample. Following the scheme in Fig. 8, sections from the 3D reconstructed volume of the crack samples are displayed in Fig. 9.

In a 3-point bending test, considering a homogeneous sample, the crack initiation is theoretically known to be exactly under the middle-upper support where the moment is maximum. The crack will propagate, from the bottom surface in tension

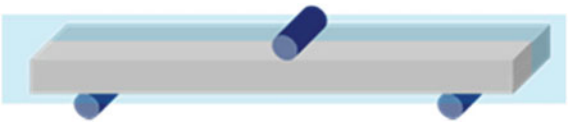

Fig. 8 Representation of a vertical section in the sample

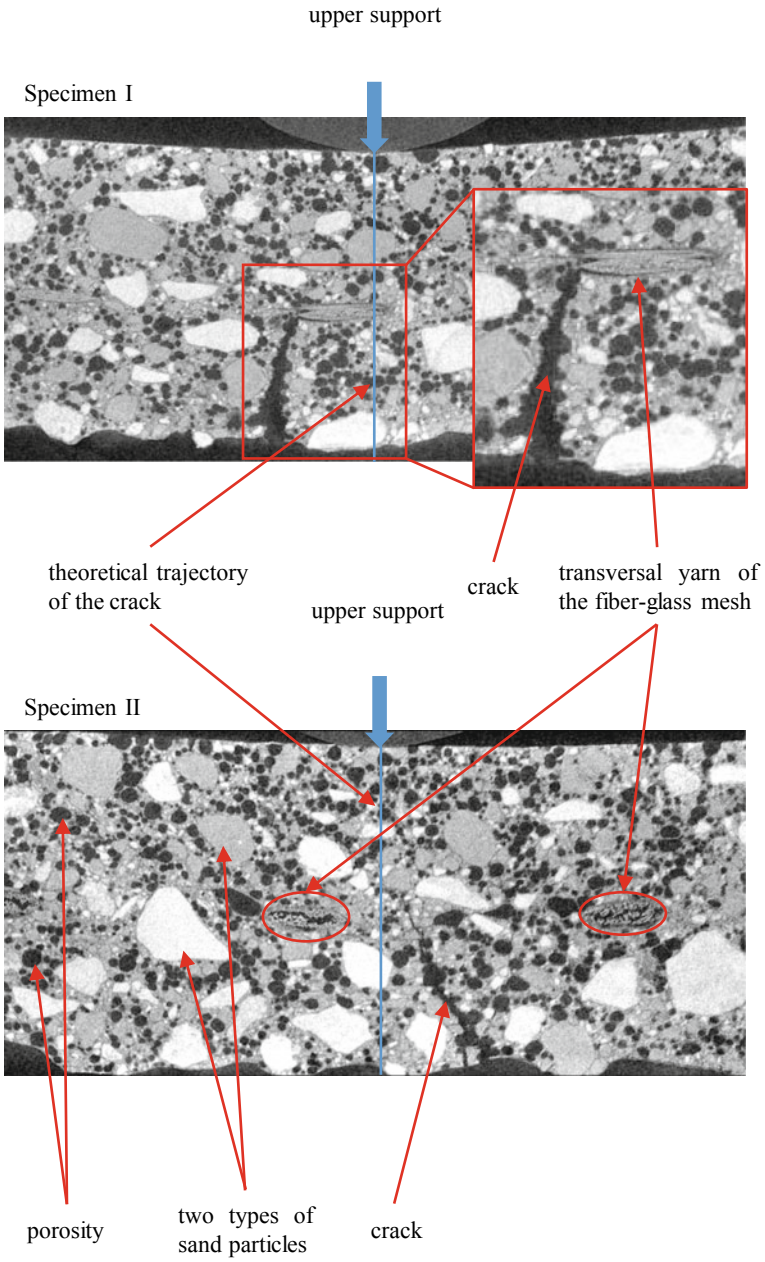

Fig. 9 Vertical sections inside the reconstructed 3D volumes of cracked specimens I and II

toward the upper surface, vertically due to the geometrical and mechanical symmetry of the classical 3-point bending set-up.

This theoretical cracking pattern is not obtained in our 3-point bending tests. The crack trajectory is neither located under the middle-upper support nor vertical. It is slightly shifted from the center and inclined as shown in Fig. 9.

3.2 Study of the Cracking

The theoretical cracking trajectory described above does not always apply to heterogeneous materials, since the heterogeneities present in the material may induce geometrical singularities, weak points, or, material incompatibilities that can relocate the crack initiation and redirect its propagation. In the reinforced fiber-glass mortar samples, three main categories of heterogeneities exist at the millimeter scale: (macro)porosity, sand particles (two types of sand can be differentiated), and, the fiber-glass mesh. Each of these heterogeneities can be a source of stress concentration.

Considering the heterogeneities as inclusions in the tensile zone, stress concentration, as well as crack trajectory, will be as shown in Fig. 10. Therefore, several phenomena are to be considered to determine the crack initiation. The crack in the mortar is initiated where the local stress attains the mortar's tensile strength, hence anywhere in the tensile zone and not only on the lower surface of the sample as in homogeneous materials.

Considering the quasi-brittle behavior of the mortar, the propagation of the crack once initiated is rapid. Since the X-ray 3D requires a steady-state of the scanned object hence cannot be carried out during the mechanical test but afterward, the exact location of the crack initiation cannot be determined. The vertical sections shown in Fig. 9 show the critical influence of the porosity on the trajectory of the crack: it is clear how the crack preferentially passes through several porosities on its way up. The fiber-glass fabric plays an important role as well.

The cracks in both samples of Fig. 9 did not cross the fiber-glass mesh. The latter stops the crack propagation and thus limits the crack opening. This first reinforcement mechanism directly influences the durability of the ETICS. As discussed in the introduction, the potential water leakage is limited by the smaller crack opening. In the reinforced mortar, emerging cracks should not easily attain the thermal insulator since they do not propagate through the entire thickness of the mortar.

Further, the analysis of specimen I of Fig. 9 suggests a potential influence of the transversal yarn on the localization of the crack. Nevertheless, it is difficult to presume, based on the 3-point bending test, that the transversal yarn will locate the cracking in the mortar because of the maximal bending moment in the middle of the sample. This potential mechanism that will be further investigated using 4-point bending and/or tensile tests might have a relevant impact on the cracking pattern. It is thus possible, using different dimensions of the fiber-glass mesh, to directly impact the number of the cracks as well as their openings to make them less visible

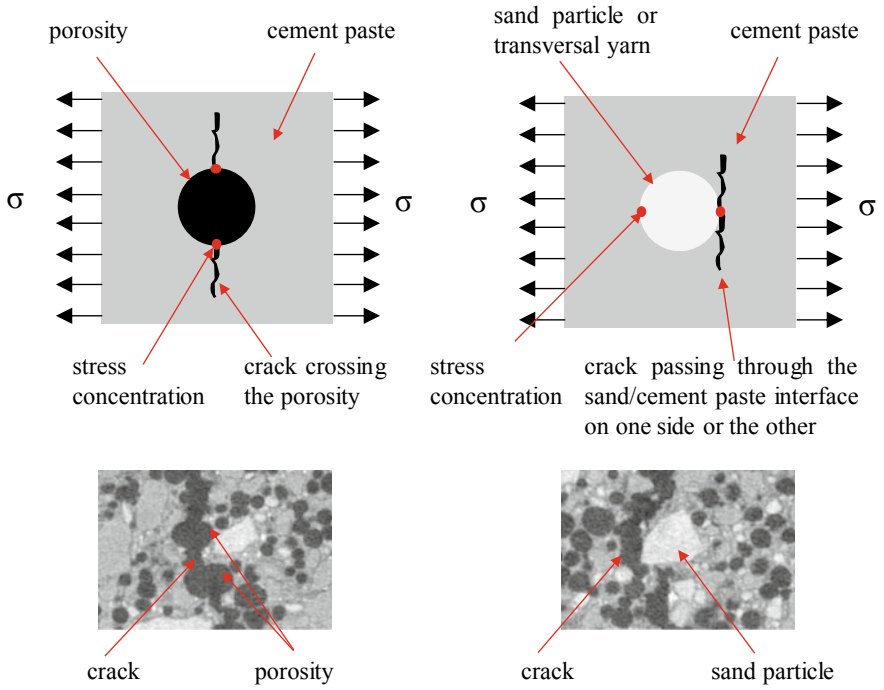

Fig. 10 Representation of the stress concentration caused by the heterogeneities in the mortar and thus the potential crack initiation and/or propagation

and more watertight. Other works investigated the influence of the fiber-glass mesh dimensions under different conditions on the mechanical behavior of the reinforced rendering mortar [12], only 2D surface observations were reported.

4 Conclusions

We studied cracking development in the reinforced mortar relevant for ETICS application using X-ray tomography. The classical mechanical testing methods even when combined with advanced technologies such as Digital Image Correlation (DIC) can only provide information on the chosen 2D surfaces. Therefore, to access the 3D information and dive into the depth of the 3D volume of the sample, a new testing setup is demanded. The newly developed X-ray in-situ inclined 3-point bending setup needed to ensure relatively small scale testing in order to obtain a sufficiently small image resolution (10 μm), X-ray transparency of the different parts of the set-up as well as geometrical adjustments in order to limit the noises and obtain good quality exploitable images.

The 3D images of the samples revealed a material crowded with different types of heterogeneities. Each of which can have an impact on the cracking pattern. Thus, the theoretical cracking pattern in a 3-point bending test is changed. The crack that should have appeared vertically in the middle of samples is shifted and inclined. This observation is mainly due to the competition between several phenomena; the maximal bending moment in the middle of the sample, the stress concentration induced by the heterogeneities in the mortar, the presence of the transversal yarn, and the real thickness of the mortar beneath the fiber-glass fabric caused by an uneven and coarse lower surface.

Although the initiation point of the crack could not be identified, two main observations have been made. First, the porosities and the sand part particles will dictate the trajectory of the crack. The crack will pass through the porosities and encounter the sand particles on its way up towards the fiber-glass mesh. Second, the fiber-glass mesh will stop the propagation of the crack. The crack will not propagate through the entire thickness of the mortar, thus limiting its opening. Therefore, the fiber-glass mesh plays an important role in the durability of the ETICS by reducing the potential water leakage within the thermal insulator.

Note that, using the 3D images, we can have access to the width of the crack opening, not only on the surface but through the length of the crack using Digital Volume Correlation (DVC).

As stated above, the transversal yarn of the grid, whether it is a warp or a weft yarn, might influence the localization of the crack. This assumption is to be further investigated along with the influence of other heterogeneities. X-ray in-situ 4-point and/or tensile tests will be carried out. The advantages of 4-point bending compared to 3-point, is the constant bending moment between the upper supports, thus limiting the competition between the transversal yarn and the maximal bending moment in the 3-point bending.

On the other hand, in order to identify the starting point of the crack and to ensure whether it initiates on the tensile surface or by one of the heterogeneities especially the transversal yarn, 2D X-ray radiography along with the 4-point bending set-up might be of great use.

In future studies, experiments will be carried out to understand the cracking behavior and the reinforcement mechanisms under the real environmental loading. Temperature and relative humidity fatigue cycles can be applied to a defined structure of ETICS. This environmental loading supported by an imaging technique can reveal the behavior of the fiber-glass reinforced mortar in “real-life” scenarios.

References

1. iea, Tracking Building. https://www.iea.org/reports/tracking-buildings-2020 (2020). Last accessed 2 Sept 2020
2. Ministry of ecological solidarity transition, Energy renovation of buildings: A plan to accelerate general mobilization. https://www.ecologique-solidaire.gouv.fr/renovation-energetique-

des-batiments-plan-accelerer-mobilisation-generale. Last accessed 2 Sept 2020 (in French)
3. Government, Press file: France relaunch. https://www.gouvernement.fr/sites/default/files/document/document/2020/09/dossier_de_presse_france_relance_-_03.09.2020.pdf. Last accessed 1 Sept 2020 (in French)
4. Barreira, E., de Freitas, V.P.: External Thermal Insulation Composite Systems (ETICS): An Evaluation of Hydrothermal Behavior. Springer (2015)
5. Eurorean Association for External Thermal Insulation Composite Systems, About ETICS. https://www.ea-etics.eu/etics/about-etics/. Last accessed 2 Sept 2020
6. Amaro, B., Saraiva, D., de Brito, J., Flores-Colen, I.: Inspection and diagnosis system of ETICS on walls. Constr. Build. Mater. **47**, 1257–1267 (2013)
7. Nilica, R., Harmuth, H.: Mechanical and fracture mechanical characterization of building materials used for external thermal insulation composite systems. Cem. Concr. Res. **35**(8), 1641–1645 (2005)
8. Pareira, C., de Brito, J., Silvestre, J.D.: Contribution of humidity to the degradation of façade claddings in current buildings. Eng. Fail. Anal. **90**, 103–115 (2018)
9. Chan, N.: Effects of initial stresses and strains in the prediction of cracking and failure of concrete structures by a discrete element approach, Ph.D., Paris-Saclay University, to be submitted (2021) (in French)
10. Chilwesa, M., Facconi, L., Minelli, F., Reggia, A., Plizzari, G.: Shrinkage induced edge curling and debonding in slab elements reinforced with bonded overlays: influence of fibers and SRA. Cement Concr. Compos. **102**, 105–115 (2019)
11. Chen, Y.: Damage mechanisms of SiC/SiC composite tubes: three-dimensional analysis coupled with tomographic imaging and numerical simulations, Ph.D., Paris-Est University (2017) (in French)
12. Colombo, I.G., Magri, A., Zani, G., Colombo, M., di Prisco, M.: Textile reinforced concrete: experimental investigation on design parameters. Mater. Struct. **46**, 1953–1971 (2013)